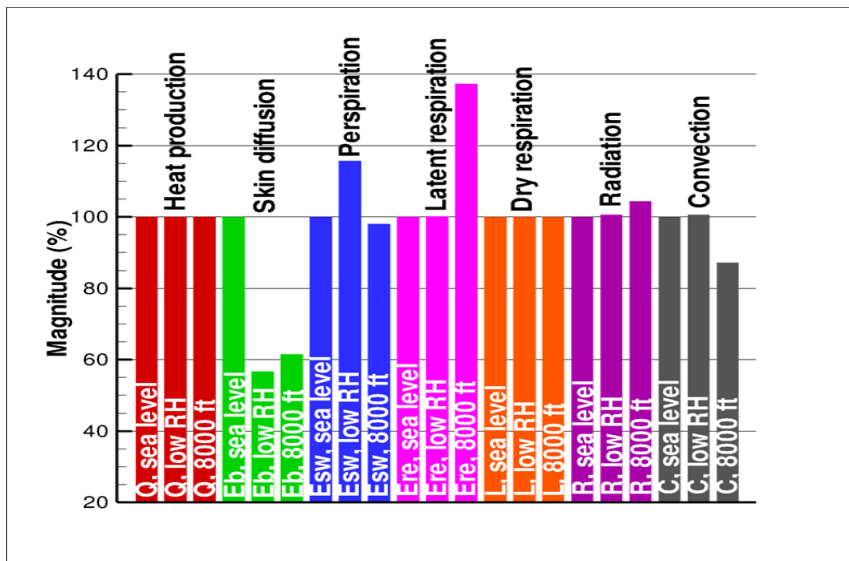




Executive summary

Modelling the impact of aircraft cabin pressure and humidity on thermal comfort



Problem area

In the second edition of the Strategic Research Agenda (SRA) of the Advisory Council for Aeronautics Research in Europe (ACARE), the research needs of Europe in the field of air transport systems over the next 20 years are outlined. One of the high level target concepts in this SRA is the highly customer oriented air transport system, and one of the key technologies of this target concept is personalized passenger climate control as part of the on-board environmental control system of future aircraft. In modern wide-body aircraft, the spacious interior allows for improved seating conditions. At the same time,

airlines operating the aircraft have their own conditions on cabin layout and interior usage. This customer-centered approach is posing significant challenges to the interior designers. Despite varying interiors within the same type of aircraft, the cabin needs to be refreshed within a given time without compromising thermal comfort for each passenger and without compromising the highly important air filtration requirements to minimize health risks. To design such cabin interiors, a level of physical modelling higher than usual is necessary, incorporating modelling upgrades from one-dimensional to three-dimensional methodology.

Report no.
NLR-TP-2010-608

Author(s)
J. van Muijden

Report classification
UNCLASSIFIED

Date
March 2011

Knowledge area(s)
Computational Physics en theoretische aërodynamica

Descriptor(s)
Cabin pressure
Relative humidity
Thermal comfort
Aircraft cabin
Predictive model

This report is based on a presentation held at the 40th International Conference on Environmental Systems ICES-2010, Barcelona, Spain, 11-15 July 2010.

Description of work

In the framework of the European Ideal Cabin Environment (ICE) project, the enhancement of the Tanabe thermoregulation model with cabin pressure and relative humidity dependency has been performed. The Tanabe thermoregulation model is a physics-based multi-node human model based on the bio-heat equation predicting temperature distributions over the passenger and heat exchange with the environment for an average passenger. The focus of the current research is the assessment of the sensitivity of the predicted results when cabin pressure and relative humidity are implemented in each relevant term of the set of bio-heat equations. For this purpose, a large amount of literature research has been performed to identify appropriate modelling for those terms that are susceptible to pressure variations and humidity influences. To validate the enhanced model, a significant amount of existing experimental conditions has been simulated and compared with available experimental results. Specifically, the experimental results from the ICE project using simulated flights in a depressurized flight test facility have been used to support the sensitivity conclusions for pressure and relative humidity variations from the simulated results.

Results and conclusions

A fully enhanced thermoregulation model has been obtained, following the theoretical derivation of

pressure and humidity influences for specific terms of the set of bio-heat equations. Simulated results from the enhanced thermoregulation model compare quite well with a significant amount of experimental datasets, both in terms of objective data (skin or clothing temperatures) and subjective data (thermal comfort votes). It has been found that the counteracting impact of pressure and humidity in different terms of the set of equations results in an overall limited impact of these effects on simulated results, at least for the allowable range of variations of pressure and humidity in an aircraft cabin, although a small increase of thermal comfort votes with higher cabin altitude is predicted. These findings are supported by experimentally obtained correlations. However, the shift of heat exchange between the passenger and the environment to different mechanisms can result in a change of perception of well-being of passengers, such as sensations of dry mouth and changes in perspiration.

Applicability

The enhanced thermoregulation model is readily applicable to support studies related to the definition of the optimum range of cabin environmental parameters, e.g. ventilation optimization and air recirculation, either as a stand-alone thermal comfort indicator or in a coupled mode with a CFD-method for cabin air flow.



NLR-TP-2010-608

Modelling the impact of aircraft cabin pressure and humidity on thermal comfort

J. van Muijden

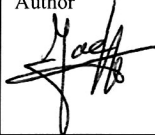
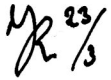
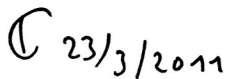
This report is based on a presentation held at the 40th International Conference on Environmental Systems ICES-2010, Barcelona, Spain, 11-15 July 2010.

The contents of this report may be cited on condition that full credit is given to NLR and the author.

This publication has been refereed by the Advisory Committee AEROSPACE VEHICLES.

Customer National Aerospace Laboratory NLR
Contract number ----
Owner NLR
Division NLR Aerospace Vehicles
Distribution Unlimited
Classification of title Unclassified
 March 2011

Approved by:

Author	Reviewer	Managing department
 23-03-2011	 23/3	 C 23/3/2011

Contents

I	Introduction	4
II	Tanabe multi-node thermoregulation model	5
III	Model enhancement for cabin pressure and humidity	7
IV	Validation of 65-node model for various applications	13
V	Conclusion	19
	Acknowledgements	19
	References	19

Modelling the impact of aircraft cabin pressure and humidity on thermal comfort

J. van Muijden¹

National Aerospace Laboratory NLR, Amsterdam, The Netherlands

In aircraft cabins during cruise conditions at high altitude, common operative values for cabin pressure and relative humidity are significantly lower than those at sea level. In this paper, the impact of cabin pressure and humidity on thermal comfort is investigated using a physics-based multi-node human thermoregulation model. The objective of developing an enhanced thermoregulation model is to support the envelope determination of environmental cabin parameters for maximum occupant well-being. Enhancements to the thermoregulation model to account for variable ambient pressure and humidity are described and applications of the model are shown. It is concluded that, within the normal operative range of aircraft cabin pressure and humidity, their impact on thermal comfort of passengers is limited.

Nomenclature

Latin symbols

B	= convective heat exchange with the central blood compartment
C	= heat capacity
c	= specific heat of dry air
clo	= unit of clothing insulation (1 clo = 0.155 m ² K/W)
D	= conductive heat exchange with neighbouring layers within a segment
E	= heat loss by evaporation
f	= response due to sensible heat loss, also clothing factor
h	= heat transfer coefficient
i	= clothing vapour permeation efficiency
I	= thermal insulation of clothing
LR	= Lewis ratio
met	= unit of metabolic activity (1 met = 58.15 W/m ²)
n	= exponent of pressure impact on convective heat transfer
PMV	= Predicted Mean Vote
PPD	= Percentage of People Dissatisfied
Q	= heat production, also heat loss to the environment
R	= heat loss by respiration, also gas constant
RH	= relative humidity (%)
t	= time
T	= temperature
TS	= thermal sensation vote
V	= air speed
\dot{V}	= pulmonary ventilation rate
w	= skin wettedness, also humidity ratio

Greek symbols

Δ	= difference
λ	= heat of vaporization of water
ψ	= response due to nonlinear coupling of skin and hypothalamus sensations

¹ Senior Scientist, Department of Flight Physics and Loads, Aerospace Vehicles Division, P.O. BOX 90502, 1006 BM Amsterdam, The Netherlands, AIAA Member.



Subscripts

<i>a</i>	= ambient, also air
<i>c</i>	= convective
<i>cl</i>	= clothing
<i>dry</i>	= dry air
<i>e</i>	= evaporative
<i>eq</i>	= equivalent
<i>ex</i>	= exhaled
<i>hy</i>	= hypothalamus
<i>p</i>	= at constant pressure
<i>re</i>	= latent respiratory
<i>sk</i>	= skin
<i>sw</i>	= skin wettedness
<i>t</i>	= total
<i>w</i>	= water vapour
<i>0</i>	= sea level, also neutral state

I. Introduction

IN current civil air transportation, a trend is emerging towards a larger focus on passenger satisfaction. While air travel has become an ordinary way of transportation over the past decades for many people, passengers are becoming more demanding in terms of service and comfort. Despite the large increases in air travel volume, individual passengers insist on safe, comfortable, prompt and reliable air transportation. Aircraft cabin issues play an increasingly important role in the satisfaction of passengers, ranging from basic characteristics like seat pitch and the availability of on-board video entertainment to highly complicated issues such as the quality of on-board air and the spreading of diseases. Airlines and aircraft industries are determined to provide an optimal cabin environment in their modern fleet of aircraft that fulfills the diverse demands of individual passengers and the general regulations imposed by aviation authorities. General regulations for the aircraft cabin environment are reviewed regularly, and work is ongoing in defining new standards^{1,2}. As part of the air travel experience, passenger thermal comfort is one significant aspect in cabin-related issues.

In the framework of studying human thermal comfort for given ambient environmental conditions, activity level and other boundary conditions such as clothing, a significant amount of research has been devoted to the development of predictive models. Predictive models for thermal comfort generally simulate the interaction between the human body and the environment on the basis of some form of heat exchange equations. The output data of a predictive model typically consists of two different parts, an objective and a subjective part. The objective part consists of predicted physical values such as body temperatures and heat fluxes, values that can be validated against measured data under the same environmental and boundary conditions. Secondly, a subjective part is usually generated that provides a perceptive value of human thermal comfort for the given environmental and boundary conditions.

A well-known approach following this scheme has been developed by Fanger³ and has later been adopted as an international standardization norm⁴. Fanger's approach uses a single heat balance equation between the human body and the environment. In this model, the human body has no physical dimensions and is represented by a set of data describing the average thermal state of the body. Clothing is included as a uniform property over the body. Since only the average state is given, the body can be visualized as a single node in the surrounding environment. The resulting thermal load from the single heat balance equation is linked to the human perception of thermal comfort using a thermal sensation coefficient. The thermal sensation coefficient has been derived by correlating the mean thermal comfort votes of a group of people to the physical output of the heat balance equation. From Fanger's research, the well-known thermal comfort indices Predicted Mean Vote (*PMV*) and Percentage of People Dissatisfied (*PPD*) have emerged. Although simple in its approach and very successful in its application to e.g. building research, a number of weak points are inherent in Fanger's model. The single heat balance equation only generates averaged values of thermal comfort in a uniform environment, creating doubtful results in asymmetrical conditions like in moving vehicles with significant asymmetrical solar heat radiation through windows from one side. The model provides a perceptive qualification of the thermal environment in a single number, again based on a uniform assumption of the environmental conditions. Also, common human active regulation reactions to cold (shivering) or hot (perspiration) environments are not explicitly modelled, resulting in a limited applicability of the approach to moderate thermal environmental conditions only (i.e. approximately 20-30 degrees Celsius).

Multi-node models are better suited in dealing with more complex thermal situations. The development of multi-node models involves the subdivision of the human body in spatially distributed segments (like head, legs, arms, hands, etc.) and a number of layers per segment (like skin, fat, muscle, core). By drawing up the heat balances between adjacent nodes, a set of equations is obtained that can be solved to obtain the temperature distribution over the nodes. Active control mechanisms of the human body – i.e. shivering to produce more heat, perspiration to dump excessive heat, and related physiological reactions such as vasoconstriction and vasodilatation controlling the blood flow through the skin layer – are modelled explicitly, and have a significant impact on the output of the model. A multi-node model generates temperature distributions on the body or on the passenger's clothing that can be verified in experiments. On the other hand, a single perceptive qualification of the ambient thermal environment is more difficult to obtain from the distributed data from multi-node models, although correlations with mean votes have been derived. A more general comfort perception analysis is to identify the well-being per body surface node by comparing the actual body surface node temperature with a preferred range of comfortable temperatures for that specific node.

A missing link in many thermal comfort models is the ability to correctly simulate the impact of varying environmental pressure and relative humidity. For aircraft cabin environments, the operational range of ambient pressure and relative humidity along the flight path is significantly different from ambient values at sea level. In the following, the enhancement of a multi-node human thermoregulation model with combined pressure and relative humidity dependency is addressed, based on physical considerations.

The main objective of developing a reliable predictive model for thermal comfort in air transportation is its application in determining the envelope of environmental cabin parameters for maximum occupant well-being, thereby supporting the development of the flying experience of the future.

II. Tanabe multi-node thermoregulation model

In the past 40 years or so, a significant amount of research has been devoted to the development of models to determine the thermal state of human beings under different environmental conditions, including their perception of thermal comfort. Resulting thermal comfort models range from simple one³ or two-node⁵ models to multi-node models, where 'multi' is to be interpreted as at least an order of magnitude larger than one. During this entire period, the development of multi-node human thermoregulation models has been attempted⁶. Such models simulate phenomena of human heat transfer inside the body and at its surface, taking into account the anatomical, thermal and physiological properties of the human body. These multi-segmental and multi-layered models are capable of predicting local temperatures in each node. The environmental heat losses are determined on the basis of resulting inhomogeneous distribution of temperatures over the body.

In the present work, the multi-node model of professor Tanabe⁷ is taken as the starting point. Tanabe's model is an advanced and yet compact multi-node thermoregulation model, which has been developed as an extension of the model of Stolwijk⁶. The model of Stolwijk consists of six body segments, each with four layers of tissue, which together with a central blood compartment results in a 25-node model. A draw-back of the Stolwijk model is its inherent symmetry, i.e. no distinction between left and right hand and so on, rendering the Stolwijk model unsuitable for asymmetrical environmental conditions. In the extension of this model by Tanabe, more nodes are used without symmetry assumptions. Use is made of sixteen separate body segments, i.e. head, chest, back, pelvis, left and right upper arm, left and right lower arm, left and right hand, left and right upper leg, left and right lower leg, and left and right foot. In Fig. 1, a schematic representation of the Tanabe model anatomy is shown. Similar to the Stolwijk model, all sixteen body segments consist of the same, concentric four layers

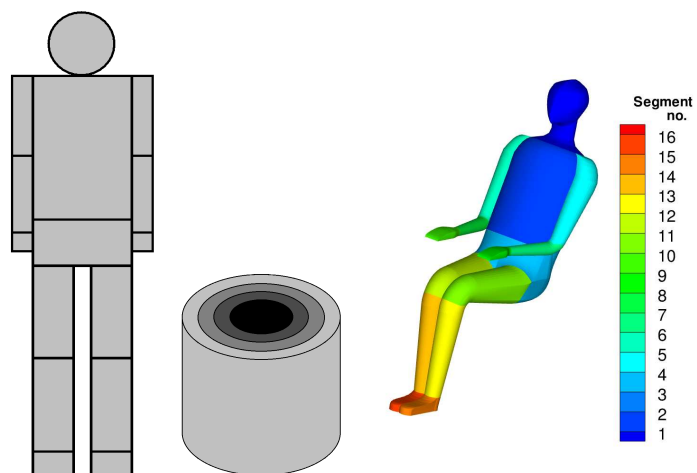


Figure 1. Body segmentation in the 65-node model, consisting of 16 body segments (left), each having 4 layers of different tissue (middle). For visualization of model results, a seated manikin can be used (right), currently showing the numbering of segments.

per segment with a similar tissue distribution. In this way, together with a central blood compartment, a 65-node model is obtained. The model replicates an averaged man with respect to body mass of 73 kg and a total body surface area of 1.87 m². For the Tanabe model, the total body surface area and its distribution over the six main body elements are quite similar to the values as used by Stolwijk.

The thermoregulation model consists of a passive and an active system part. By modelling the physical human body and the heat transfer phenomena occurring inside and at its surface, the passive system is obtained. For each of the 65 nodes, the heat transfer phenomena are represented by a time dependent heat balance equation (also known as bio-heat equation), which takes the general form:

$$C \frac{dT}{dt} = Q - B + D - R - E - Q_t \tag{1}$$

Here, C represents the heat capacity of each node, T is its temperature, and t is the time. On the right hand side, Q denotes the heat production, B represents the convective heat exchange with the central blood compartment and D accounts for conductive heat exchange with neighbouring layers within the same segment. The term R represents the heat loss to the environment by respiration, occurring only at the core layer of the chest. The respiration heat loss to the environment is the sum of the dry respiration heat loss due to warming of the inhaled air, and of the latent respiration heat loss related to evaporation of moisture in the lungs which increases the relative humidity of the inhaled air. The term E , active in the skin layer only, accounts for the evaporative heat loss, and Q_t is the sum of the

convective and radiant heat exchange to the environment. Both these terms are influenced by the clothing the passenger is wearing. The heat balance in the central blood compartment accounts for convective heat exchange with all body segments and their layers. The modelled heat exchange between nodes in the Tanabe model is depicted in Fig. 2. The rate of heat production Q on the right hand side of equation (1) consists of three different contributions, stemming from the basal metabolic rate, from heat production by external work, and from shivering. The latter two contributions occur only in the muscle layer and are zero in all other layers. Applying equation (1) to all nodes, a set of 65 equations is obtained. Solution of the set of equations is straightforward, applying time integration until a steady-state solution is obtained. The solution process requires the evaluation of the right-hand sides of the

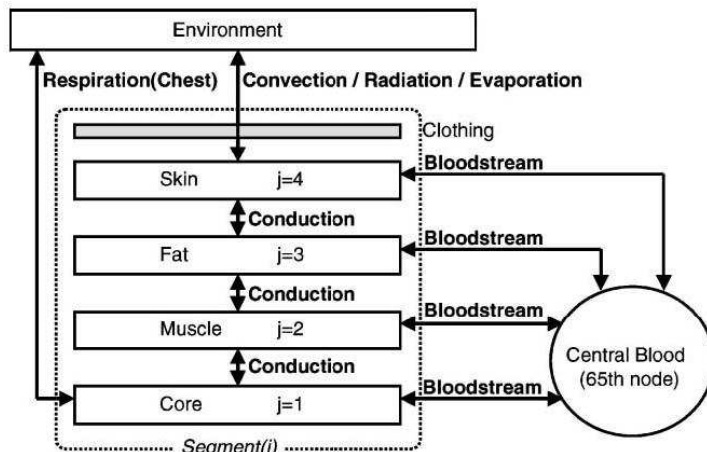


Figure 2. Conceptual model of heat exchanges between segments and layers of the Tanabe 65-node model, with i representing the body segment number (1 to 16) and j the tissue layer (1 to 4).

equations during each time step.

Some remarks have to be made here for the impact of the insulation of the human body by clothing. Two types of clothing insulation have to be considered. The overall value is defined as an insulation value of a clothing ensemble as if applied over the entire body surface, as is used in Fanger's model. However, such a value does not represent the local values which are needed in a segmental model like the 65-node model. Calculation procedures to get overall clothing values from clothing items are for example defined in Ref. 8. The unit *clo* represents the clothing insulation. A more detailed description of establishing the local insulation values for clothing ensembles is given in Park⁹. For practical purposes, five clothing ensembles for a seated person have been defined in terms of local insulation values according to this approach that are easily switched on in the 65-node model. The five clothing ensembles represent appropriate clothing insulation for the following situations: summer indoor, summer outdoor, spring/autumn, winter indoor, and winter outdoor. In these clothing ensembles, the contribution of a typical aircraft seat has been included.

The active system is represented by four different thermoregulatory mechanisms, namely: vasodilatation and vasoconstriction that are controlling the blood flow through the skin, and perspiration and shivering as active heat loss and heat production mechanisms. The active thermoregulatory mechanisms are controlling terms in the right-hand sides of the set of 65 passive equations. The active thermoregulatory mechanisms are driven by a head core signal, a skin signal, and a signal related to both (core and skin). In this context, a signal driving the rate of thermoregulation is a temperature difference between the actual node temperature and the set-point temperature. Thus, the 65-node model has predefined set-point temperatures for each node. The set-point temperatures represent the thermally neutral situation of the human body, the ideal thermal situation which is perceived as neither too warm nor too cold.

A more detailed description of the basic 65-node model, the precise form of the right-hand side terms of the set of equations, and the active control signals definitions can be found in Ref. 4. The 65-node model has been applied as a stand-alone routine, in which case the convective and radiative heat exchange with the environment is based on predefined heat transfer coefficients as averaged from thermal manikin measurements. Alternatively, the 65-node model has been coupled with the in-house CFD-system at NLR¹⁰, see Fig. 3 where a forced convection case by prescribed air input and output conditions due to the air refreshment system is shown for half a cabin slice. In this case, the convective and radiative heat transfer coefficients are calculated based on accurate geometrical and fluid flow information from the non-uniform cabin environment. Thus, the influence of the thermal cabin environment on the passenger is calculated while also the impact of the passenger acting as a heat source on cabin convection is obtained. Obviously, the coupled approach provides a larger flexibility and higher accuracy at the cost of the effort needed to model the cabin environment in a CFD-mesh.

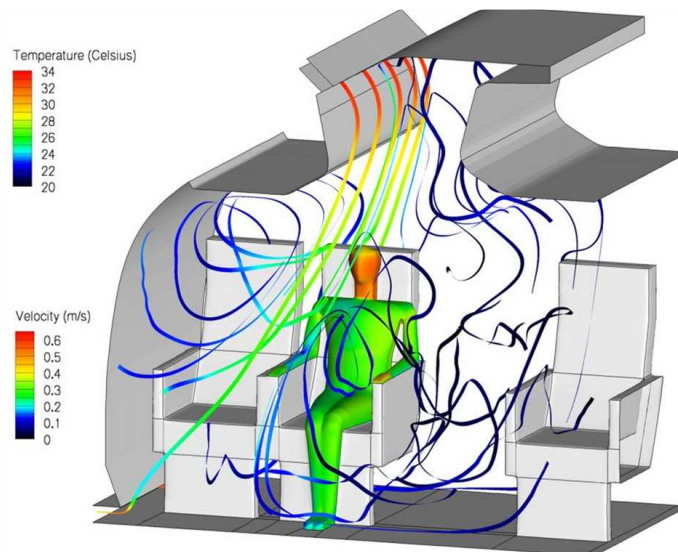


Figure 3. Coupling example of 65-node thermoregulation model in a CFD-environment for accurate determination of heat exchange with the cabin environment. Manikin surface shows actual skin/clothing temperatures, coloured streaks show recirculation zones and local air velocities of cabin flow.

III. Model enhancements for cabin pressure and humidity

Besides experimental investigations^{11,12,13} regarding cabin influences on the passengers, there is also the need for modelling the cabin influences in thermoregulation models for the sake of sensitivity analysis under varying cabin conditions. The main impact of aircraft cabin environments relative to normal vehicle or office environments at sea level is caused by the significant variations in cabin pressure and humidity. In the definition of the standard atmosphere¹⁴, the pressure variation with altitude is shown in Fig. 4. Following regulations, the cabin pressure is not allowed to drop below the value occurring at an altitude of 8000 ft, which is identical to a cabin pressure limiting ratio of 0.743.

The reduction of cabin pressure has an impact on several terms in the bio-heat balance of Tanabe's model, which will be addressed below. Also, a very low relative humidity is to be expected in aircraft cabins at cruise altitude, with usual values in the order of 5-15 percent. Such a low relative humidity is believed to affect the basal wettedness of the skin, having a normal value of 0.06 which may drop to values as low as 0.02 in very dry environments.

A. General assumptions

Lacking specific information, it is assumed that all the properties of the individual tissue in each body segment as well as the central blood compartment are independent of the air pressure. The properties represent: heat capacity, basal metabolic rate, basal blood flow, thermal conductance, density, and set-point temperatures. The dimensions, i.e. the body surface area and the weight, are taken independent of pressure as well. Furthermore, all weighting, distribution and control coefficients are independent of air pressure. Concerning the clothing, it is assumed that the air pressure does not affect the dimensions of the garments worn. Since the clothing area factor f_{cl} is defined as the

ratio between the outer surface of the clothed body and the skin surface, this factor is unchanged. Finally, the influence of air pressure on the insulation properties of the garments worn is unchanged. Note that the impact of air pressure on the vapour permeation efficiency of the clothing will be addressed below.

B. Investigations on contributions to the bio-heat equation

Evaluating the general assumptions reported above for the bio-heat equation (eq. 1), the heat capacity C , basal heat production Q , and heat production by external work W are independent of air pressure, as well as heat transfer by blood flow B and the heat exchange by conduction D . The same holds for the active terms in the thermoregulatory system, i.e. the signals controlling vasomotion, perspiration and shivering heat production. The remaining terms of the bio-heat equation are: heat loss by respiration (R), heat loss by water vapour diffusion through the skin (E), and sensible heat exchange at the skin surface due to convection and radiation (Q_s). These terms, and the influence of cabin conditions, are described below.

C. Transdermal water vapour diffusion

Skin wettedness is defined as the actual evaporative heat loss divided by the maximum possible evaporative heat loss. The basal skin wettedness is related to the transdermal skin diffusion which is a passive mechanism as opposed to perspiration. Variations of the basal skin wettedness (w_{sw}) have been re-examined in order to obtain a decreased value of the basal skin wettedness when exposed to very dry environments. The normal value of 0.06 might drop to a value as low as 0.02, depending on the actual relative humidity¹⁵ which is supported theoretically by Gonzalez¹⁶. The following linear model is proposed, creating a dependency of the basal skin wettedness on ambient relative humidity:

$$w_{sw} = \min(0.06, 0.01 + RH * 0.06 / 70). \quad (2)$$

This approach results in a basal skin wettedness value of 0.06 at a relative humidity of 58.33 percent or higher, and a linear decrease below this value until at about 10 percent relative humidity the value 0.02 is obtained. It should be noted, however, that a reduction in basal skin wettedness will be counteracted by the active regulation system through the perspiration term, if necessary. Therefore, it is believed that the actual form of the dependency of the basal skin wettedness on relative humidity is not that important.

D. Latent respiratory heat loss

The latent respiratory heat loss is modelled in the usual way³ as

$$E_{re} = \dot{V}(w_{ex} - w_a)\lambda, \quad (3)$$

where \dot{V} is the pulmonary ventilation rate, w_{ex} is the humidity ratio of the expired air, w_a is the humidity ratio of the ambient air, and λ is the heat of vaporization of water. It can be shown that the heat of vaporization of water does not change with pressure and is a function of temperature only. There is no need for specific adaptations of eq. 3 to altitude conditions, as long as unnecessary approximations are avoided. The humidity ratio of ambient and expired air is calculated directly from the common psychrometric relation

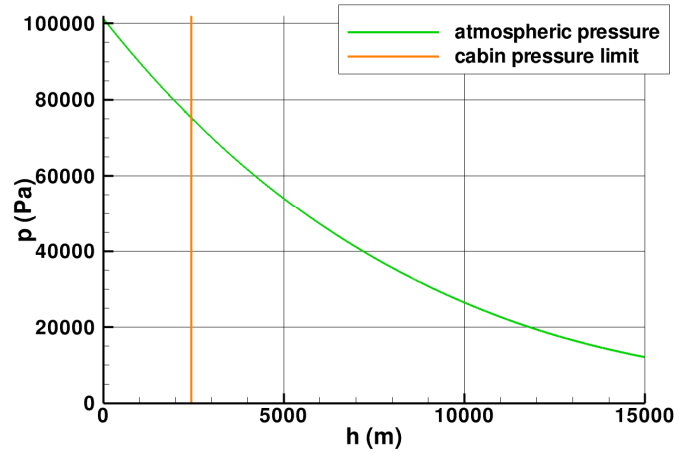


Figure 4. Atmospheric pressure as function of flight altitude. The maximum cabin altitude is defined at 8000 ft (2438 m), setting the cabin pressure limit at a minimum value of 75271 Pa.

$$w = \frac{R_a}{R_w} \frac{p_w}{p - p_w}, \quad (4)$$

with R_a and R_w denoting the gas constants for dry air and water vapour, respectively, having a constant ratio of 0.622. The pressure terms p and p_w denote the pressure of moist air and water vapour, respectively. Using the ambient and exhaled air temperature, eq. 3 can be evaluated. According to Fanger³, the exhaled air temperature is given by

$$T_{ex} = 32.6 + 0.066T_a + 32w_a. \quad (5)$$

E. Dry respiratory heat loss

No changes are necessary to account for variations in cabin conditions to the dry respiratory heat loss. The common expression³

$$E_{dry} = \dot{V} c_p (T_{ex} - T_a) \quad (6)$$

can be used as is, with c_p denoting the specific heat of dry air at constant pressure. For an ideal gas, which is a common assumption for dry air, it can be shown that the specific heat at constant pressure is independent of the ambient pressure¹⁷.

F. Convective heat loss

From common correlations in heat transfer studies between Nusselt, Reynolds and Prandtl numbers, which are obtained in a semi-empirical way by dimensional reasoning and using experimental data, a dependency of the convective heat transfer on pressure can be obtained¹⁸. The common expression for the convective heat transfer coefficient resulting from such an analysis is given by

$$\frac{h_c}{h_{c_0}} = \left(\frac{p}{p_0} \right)^n \quad (7)$$

with subscript 0 indicating sea level values. The actual value of the exponent n is variable, depending on the type of convection (natural, forced or mixed) and on the geometry used. For human bodies, the advocated powers range from 0.5 (Kreith¹⁸), 0.55 (ASHRAE, see Chang¹⁹) to values higher than 0.60 (de Dear²⁰). The actual value has some impact on overall results, see Fig. 5, but its value is not that important due to counteracting effects from other terms in the bio-heat equation that also depend on the power of the convective term. The proposed value is 0.6, which is supported from studies under extreme conditions²¹.

In case the thermoregulation model is used in a strongly coupled fashion with a CFD-model, the convective heat transfer coefficients are calculated directly from the flow solution, by relating the conductive heat transfer deep in the resolved boundary layer with the convective heat loss. In the case of using the thermoregulation model in a stand-alone mode, eq. 7 can be enhanced

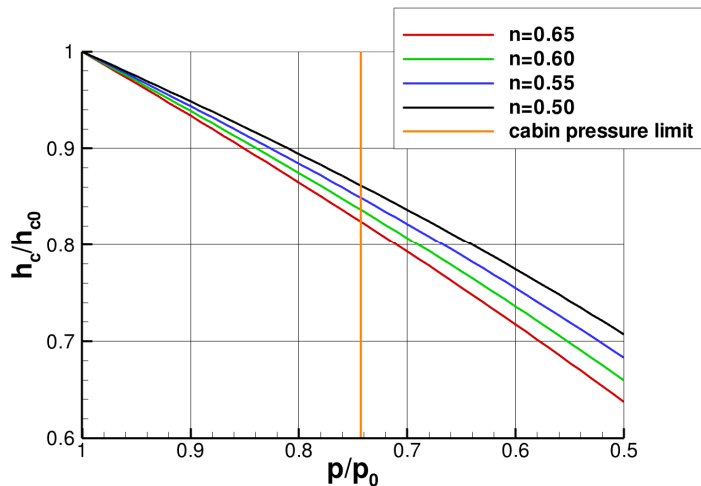


Figure 5. Relative changes in convective heat transfer coefficient with cabin pressure, showing the impact of the exponent n in still air (eq. 7).

for non-negligible air speeds (air speeds larger than 0.1 m/s) by

$$\frac{h_c}{h_{c_0}} = \sqrt{\frac{V}{0.1}} \left(\frac{p}{p_0} \right)^n, \quad (8)$$

with V denoting the convective air speed and h_{c_0} now denoting the convective heat transfer coefficient at sea level in still air.

G. Evaporation heat loss

In the Tanabe model, the evaporative heat loss from the skin is modelled by

$$h_e = \left(\frac{LR i_{cl}}{I_{cl} + \frac{i_{cl}}{h_c f_{cl}}} \right). \quad (9)$$

In this equation, LR denotes the Lewis ratio defined as the ratio of heat to mass diffusivity, i_{cl} denotes the clothing vapour permeation efficiency, and f_{cl} is the clothing area factor, i.e. the ratio of the body surface area of the clothed person to the surface area of the nude person. For a nude person (i.e. $I_{cl}=0$, $f_{cl}=1$), eq. 9 states that $h_e=LR \cdot h_c$, which is a well-known result. At sea level, the Lewis ratio is 16.5 °C/kPa or 0.0165 °C/Pa. The value for i_{cl} is usually taken as 0.45 at sea level. These values have a pressure dependency, however, as will be detailed below. When taking the correct ambient pressure impact on the convective heat transfer coefficient, on the Lewis ratio and on the garment vapour permeation efficiency, the evaporative heat transfer coefficient follows automatically. The pressure impact will be shown after defining the pressure impact on Lewis ratio and on the clothing vapour permeation efficiency.

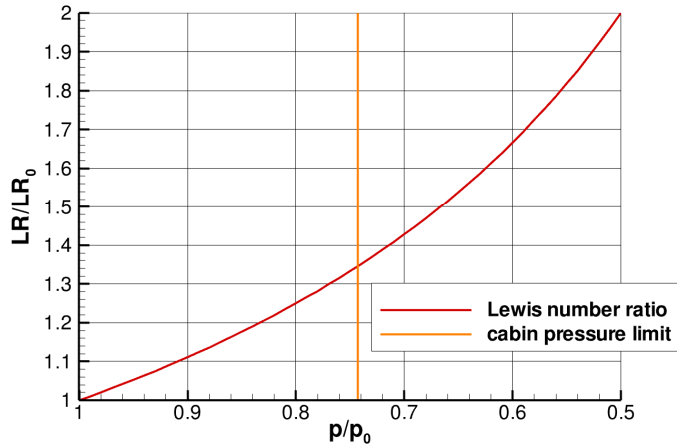


Figure 6. Impact of cabin air pressure ratio on Lewis number ratio.

H. Lewis ratio

The Lewis ratio is defined as the ratio between the Schmidt number Sc and the Prandtl number Pr . The Schmidt number describes the ratio of momentum to mass diffusivity, and the Prandtl number describes the ratio of momentum to heat diffusivity. Since the Schmidt number is inversely proportional to the density, and thus the pressure, and the Prandtl number is independent of the pressure, the following expression holds:

$$\frac{LR}{LR_0} = \frac{p_0}{p}, \quad (10)$$

with subscript 0 indicating sea level values. Thus, the Lewis ratio is inversely proportional to the pressure ratio, see Fig. 6. This equation is also found in McIntyre²².

I. Clothing vapour permeation efficiency

Different approaches regarding the garments are found in literature. Havenith²³ gives a refreshing look on some of these approaches. By combining the two approaches of ISO^{8,24} and complementing the result with the measured data from Kozak²⁵, an expression can be derived for the pressure dependency of the vapour permeation. While the data by Kozak²⁵ are given per type of cloth, the combination of data following the combination of ISO-approaches^{8,24} results in a generally valid approach, independent of the type of cloth. Using this approach, the pressure dependency is based on hypobaric as well as hyperbaric investigations and is thus expected to be consistent and valid over a wide range of pressure variations. The resulting equation is given by

$$\frac{i_{cl}}{i_{cl_0}} = \left(\frac{p}{p_0} \right)^{n+0.47} \quad (11)$$

Here, n represents the exponent as used in the convective heat transfer coefficient, see Eq. 7 and Eq. 8. As a result, the pressure dependency power in this equation is close to unity for common values of the convective power n . The variation of the clothing vapour permeation efficiency with pressure is shown in Fig. 7.

Summing up the above described pressure influences to obtain the pressure dependency on the evaporation heat loss of Eq. 9, the results are shown in Fig. 8. It is found that, relative to a nude person, the clothing significantly reduces the pressure impact on the evaporative heat transfer coefficient. Nevertheless, depending on the garments worn, at minimum cabin pressure an impact of up to about eight percent can be expected.

J. Impact of convection exponent n on predictive model results

The exponent n as used in modelling the impact of air pressure on the convective heat transfer coefficient is reported to range between values of 0.5-0.65 for human applications. The actual value of the exponent n has some impact on overall results of the model. It will be shown that this impact is of minor importance with respect to the current project objectives. For this purpose, seated reclining persons (with a metabolic rate 1.0) in an aircraft cabin environment at 8000 ft cabin altitude, i.e. at a cabin pressure of 75271 Pa, and 15 percent relative humidity at ambient temperatures of 25°C are simulated for the five available clothing profiles. As output, the average skin temperatures as predicted are given in Table 1. It is found that the resulting mean skin temperature hardly varies with the exponent n , and the variations that occur are

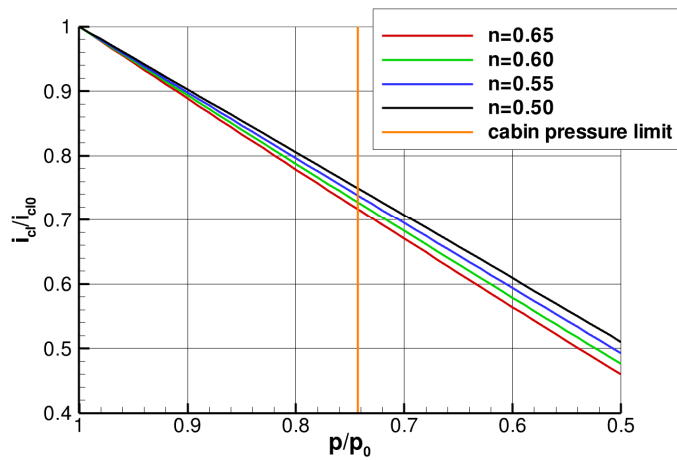


Figure 7. Impact of cabin air pressure ratio on clothing vapour permeation efficiency, for various values of the convective heat transfer exponent n .

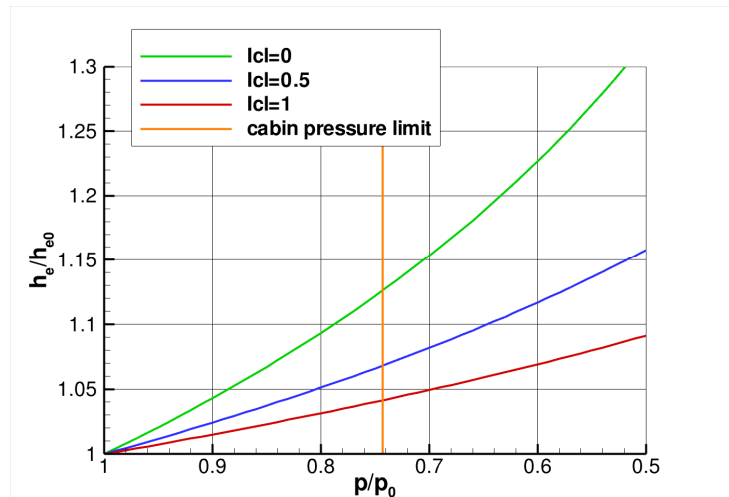


Figure 8. Impact of cabin air pressure ratio on evaporative heat transfer coefficient (using a convective exponent $n=0.6$) for nude and clothed persons

Clothing profile	nude	1	2	3	4	5
$n=0.5$	32.38	34.65	34.55	34.75	34.95	35.20
$n=0.6$	32.42	34.65	34.56	34.76	34.95	35.21
$n=0.65$	32.44	34.66	34.56	34.76	34.95	35.22

Table 1. Impact of convective exponent n on predicted mean skin temperature, at met=1.0, $T_a=25^\circ\text{C}$, RH=15%, 8000 ft cabin altitude

well within any known accuracy of experimental results. The active regulation mechanism as has been implemented in the 65-node model might play a non-negligible role in keeping these outputs at rather constant levels. Following Brake²¹, the value $n=0.6$ has been selected in the model.

K. Correlating model output to thermal comfort votes

The common output of multi-node models, i.e. the objective data for temperature distributions, can be compared directly with measured data. However, quite often the available experimental data are limited to the more subjective thermal votes. For multi-node models, specific care has to be taken to analyze and correlate the spatially distributed model output to thermal votes. In the automotive industry, it is common to compare local equivalent temperatures per body segment with certain boundaries of comfort^{26,27}. This approach is also used here to visualize the output of the 65-node model. On the other hand, an overall thermal comfort vote like *PMV* is sometimes very handy, especially when the thermal environment is only mildly deviating from comfortable conditions and not too much influenced by asymmetries. For this purpose, the approach of Fiala²⁸ is followed, although the correlation has been adjusted to the specific characteristics of the Tanabe model in order to arrive at similar thermal votes. The thermal sensation vote is obtained from

$$TS = 3 \tanh(f_{sk} + \psi). \quad (12)$$

In this approach, f_{sk} represents the response due to sensible heat loss at the skin and ψ represents the response due to the nonlinear coupling of skin and hypothalamus sensations. The current implementation is slightly different from Fiala's original correlation; the following expression is used for the sensible heat loss at the skin:

$$f_{sk} = \begin{pmatrix} 0.6 \\ 0.298 \end{pmatrix} \Delta \bar{T}_{sk} \Big|_{-}^{+}. \quad (13)$$

Eq. 13 should be interpreted such that when the temperature difference $\Delta \bar{T}_{sk}$ is positive, the upper multiplying coefficient is used and alternatively the lower coefficient should be applied. The expression for the nonlinear coupling of skin and hypothalamus sensations is given by

$$\Psi = 6.662 \exp\left(\frac{-0.565}{\Delta T_{hy}}\right) \exp\left(\frac{-7.634}{5 - \Delta \bar{T}_{sk}}\right). \quad (14)$$

The temperature differences in these equations are computed from actual temperatures minus the set-point temperature at thermal neutrality, corrected to improve the correlation of overall thermal vote predictions from the 65-node model with experimental data. The following expression is used for the skin temperature difference:

$$\Delta \bar{T}_{sk} = \bar{T}_{sk} - (\bar{T}_{sk, optimal} + 0.1875), \quad (15)$$

whereas the hypothalamus temperature difference is obtained from

$$\Delta T_{hy} = T_{hy} - (T_{hy, optimal} + 0.128). \quad (16)$$

IV. Validation of 65-node model for various applications

The enhanced 65-node thermoregulation model has been applied in stand-alone mode to predict the thermal comfort of people wearing various clothing ensembles in different environmental conditions, and the model output has been compared with available experimental data. For this purpose, experimental data have been used from published experiments as well as from newer experiments conducted in the framework of the Ideal Cabin Environment (ICE) project. It should be kept in mind, though, that publications sometimes poorly describe the environmental conditions, clothing ensembles of test persons, and average characteristics of the test persons like weight, height, etc. Comparisons on the basis of estimated environmental conditions and clothing profiles depend on the correctness of such information, while averaged personal characteristics determine if the current 65-node model implementation is adequate for that group. In the following, predicted results using the 65-node model are validated with objective data – i.e. measured temperatures – as well as with subjective thermal votes.

A. Validation with objective data

Though not representative for aircraft cabin environments, data from nude persons are valuable for the validation of thermoregulation models. Results for nude persons are not influenced by estimates for clothing properties. A first set of available data for a nude person is obtained from Boregowda²⁹, in which nude persons are exposed to two rather cold conditions. Available experimental data are limited to core and averaged skin temperatures. The simulated results versus experimental results are given in Table 2. Despite the remaining differences in absolute levels of temperatures between simulation and experiment, the trends observed between the two different conditions are remarkably similar from experiment and simulation.

T_a (°C)	T_r (°C)	RH (%)	Activity level (met)	T_{core} (°C) simulation	T_{core} (°C) experiment	\bar{T}_{sk} (°C) simulation	\bar{T}_{sk} (°C) experiment
13.0	13.0	45.0	1.0	35.94	36.8	27.57	26.3
17.55	17.55	30.0	1.0	36.03	36.9	29.32	28.0

Table 2. Comparison of simulated results versus experimental data for a nude person

A second set of results comprising segmental skin temperatures is found in Arens¹⁵, for neutral, warm and cold conditions. Such distributions allow for a more detailed comparison. It should be remarked, though, that the experimental conditions and clothing data are not quoted precisely. Simulations have been performed with as good as possible estimates for the required input data to obtain a close match in average skin temperature comparison. Then, the resulting body segmental temperatures have been plotted against the experimental distribution.

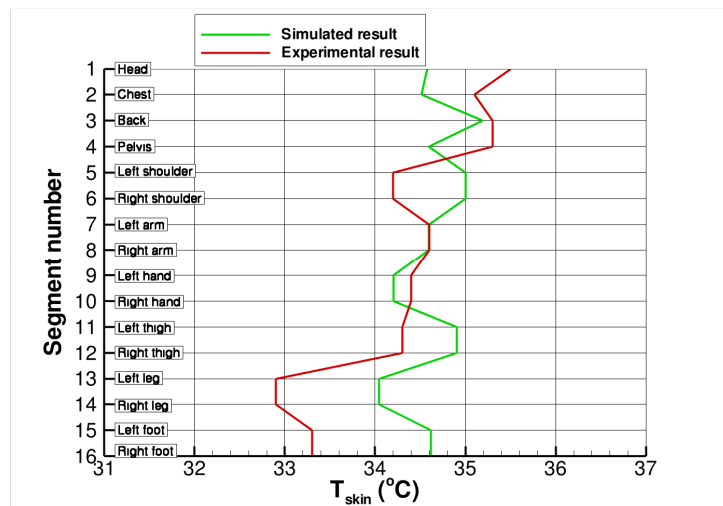


Figure 9. Comparison of segmental skin temperatures in neutral conditions.

The results for the neutral condition are shown in Fig. 9. For this case, it is estimated that the ambient and mean radiant temperature are 25°C, and that the metabolic activity equals 1.2 met. For clothing properties, a clothing profile for summer indoor has been selected, whereas the relative humidity is estimated at 50 percent. The resulting simulated and experimental average skin temperatures are 34.67°C versus 34.45°C. Despite the uncertainties in experimental conditions, it is shown in Fig. 9 that a reasonable comparison in body temperature distribution is obtained, although the legs are not as cold as in the experiment. Results for the warm condition are shown in Fig. 10. For the simulation of

this case, the temperature is estimated at 30°C, with a high relative humidity of 90 percent, a slightly higher metabolic activity of 1.4 met, and a clothing profile for summer indoor. A reasonable comparison with measured data is obtained. Results for the cold condition are depicted in Fig. 11. Once again, estimated conditions have been

used, with a temperature of 10°C, a low relative humidity of 20 percent, and a metabolic rate of 1.2 met. The persons in this test appear to be practically nude, all other clothing profiles result in higher skin temperatures. Overall, the comparisons in neutral, warm and cold conditions show a reasonable agreement between simulation and experiment. Further comments on the remaining differences would require a better knowledge of the environmental conditions of the experiment.

A third, well-documented case for comparisons is obtained from Van Ooijen³⁰, quoting core temperatures and mean skin temperatures from climate chamber experiments. In these experiments, the subject wore garments with an insulation value of 0.71 clo, which corresponds approximately to the clothing profile for summer outdoor. The test persons were reclining (metabolic activity level of about 0.8 met) during the experiments in the climate chamber. Since the experiments have been conducted in summer as well as in winter, comparisons have been made with the averaged results of both seasons. In Table 3, the results of the simulations are compared with the experimental data. It is observed that for the neutral case, averaged skin temperatures are predicted very well at a slightly too low core temperature, whereas for the cold case the prediction of the averaged skin temperature is slightly too high at a too

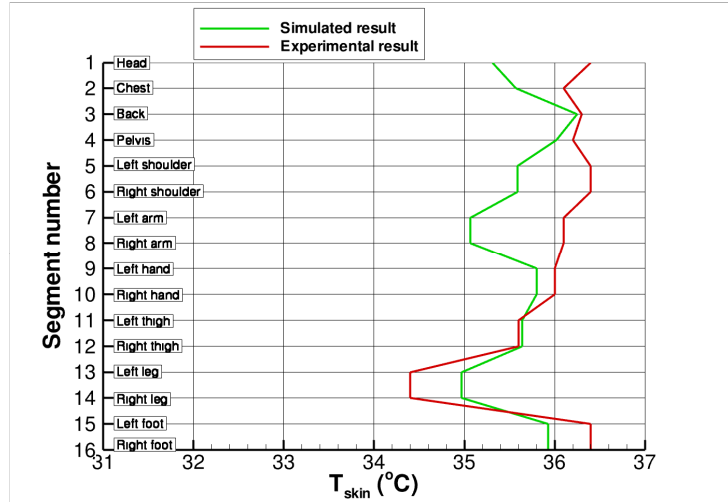


Figure 10. Comparison of segmental skin temperatures in warm conditions.

T_a (°C)	T_r (°C)	RH (%)	Activity level (met)	T_{core} (°C) simulation	T_{core} (°C) experiment	\bar{T}_{sk} (°C) simulation	\bar{T}_{sk} (°C) experiment
21.7	21.7	50.0	0.8	36.53	36.85	32.20	32.25
15.5	15.5	50.0	0.8	36.29	36.90	30.40	29.50

Table 3. Comparison of predicted skin and core temperatures with climate chamber data (averaged from winter and summer experiments)

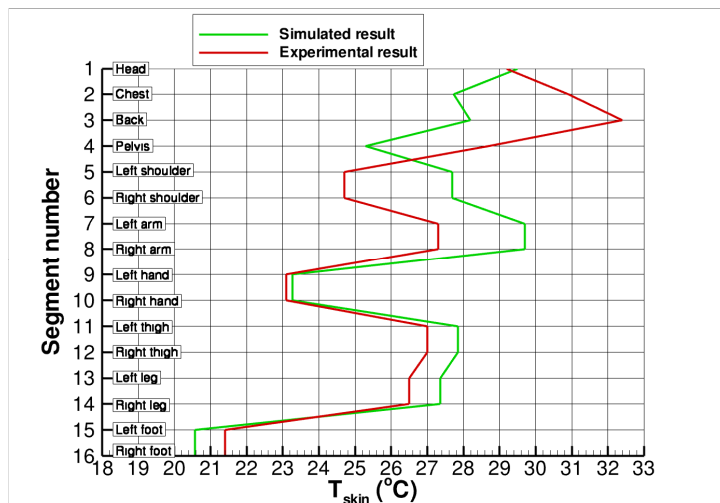


Figure 11. Comparison of segmental skin temperatures in cold conditions.

low core temperature. No effort has been devoted to study the differences between summer and winter experimental temperatures of the test persons, since the 65-node model does not distinguish seasonal variations.

A final case for comparisons is taken from Fiala³¹, where segmental temperature data are given as well as body core temperatures. The conditions for this case are for test persons clothed in a college uniform with an insulation value of 0.6 clo, exposed to a temperature of 25.5°C. For this clothing profile which is not available in the five standard clothing profiles, an additional clothing insulation distribution has been used. For this case, the simulated core temperature is 36.68°C versus an experimental value of 36.9°C. The averaged skin temperature comparison shows a simulated value of 34.10°C against an

experimental value of 33.5°C. The results are shown in Fig. 12, showing a good comparison with experimental data

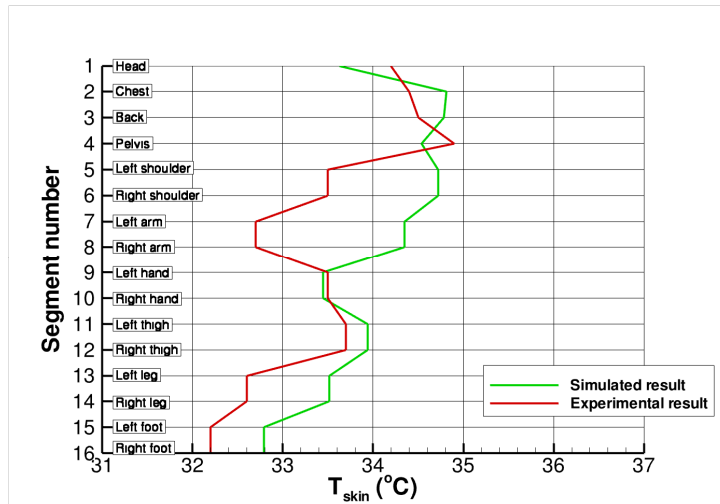


Figure 12. Comparison of segmental skin temperatures at ambient temperature of 25.5°C, clothing insulation of 0.6 clo.

except for the arms and shoulders. Probably, the clothing profile for this case needs some revision in this respect. For most segments, the predicted temperatures are slightly too warm, except for the head which is somewhat too cold.

These comparisons with objective data involve uncertainties commonly involved in the experimental temperature data due to the standard deviation of measured skin temperatures on multiple test persons, and in the actual clothing insulation distribution. For cases where the differences with experiment are significantly larger than the average, the uncertainties in input data are also larger. The conclusion is that the current thermoregulation model gives sufficiently accurate overall results and temperature distributions for steady state situations.

B. Validation with subjective data

The correlation that is applied between temperature distributions and thermal votes has already been explained. In this section, averaged actual votes are compared with predicted thermal votes. A range of experimental thermal votes for various environmental conditions and metabolic rates are taken from two different sources, Fiala²⁸ and Nilsson³².

The environmental conditions in these experiments range in temperature from 15°C to 48°C, in metabolic rate from 1 met to 4 met, and in relative humidity from 40 to 85 percent. The comparison between simulated and experimental thermal votes is shown in Fig. 13. Ideally, the comparison should show that all data points coincide with the straight line from the left lower to the right upper corner. Several outliers are identified that could be related to one of the following causes: very high metabolic activity (up to 4 met) where differences between predicted and experimental votes are observed to be more significant; non-negligible scatter in experimental data resulting in inaccurate experimental votes; and seasonal influences on experimental thermal votes. As noted before, the 65-node model does not distinguish seasonal influences and this does not appear to be of importance for the distributed temperature

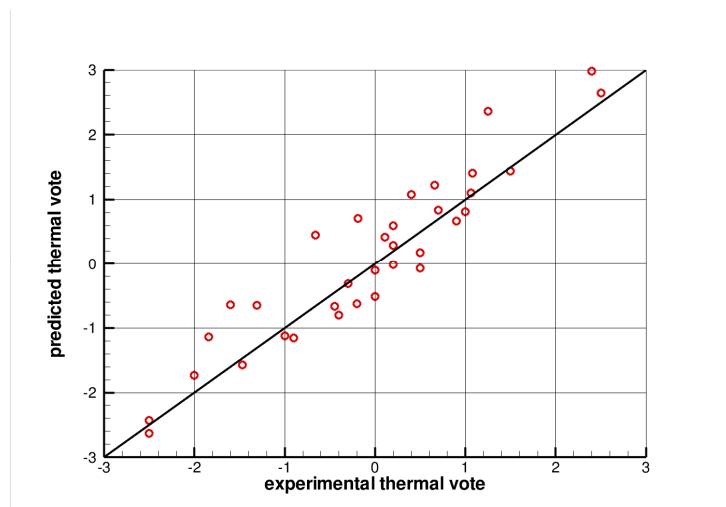


Figure 13. Comparison of 65-node model predicted thermal votes with experimental thermal votes for a wide range of temperatures and metabolic rates.

output of the model which generally shows similar comparisons with experimental data. The translation of thermal output to comfort votes, however, might benefit from seasonal influences in the correlations. Several indications exist for a non-negligible impact of the season on experimental thermal votes^{32,29,33}, although the associated objective data do not need to show a similar shift of magnitude. Apparently, during summer people tend to accept warmer temperatures as a neutral thermal condition, whereas in winter the neutral condition is found at somewhat lower temperatures. Thus, with some caution it can be stated that the temperature output of the thermoregulation model is adequate for all seasons, whereas the perception of the environmental conditions and the translation into a mean vote could be susceptible to seasonal influences.

C. Pressure and relative humidity impact

Finally, the variation of pressure and relative humidity on aircraft cabin comfort is investigated in some more detail on the basis of experiments performed in the framework of the ICE project. Temperature recordings on people during the tests were obtained using an infrared camera. The influences of cabin pressure and relative humidity, however, do not show up in skin and clothing temperature distributions obtained in this way. The resulting accuracy for the infrared recordings is quoted to be $\pm 2^\circ\text{C}$, whereas the 65-node thermoregulation model predicts skin and clothing temperature changes for aircraft cabins that are at least an order smaller than this accuracy. This is shown by a simulation of the thermal comfort of people in an environment of 23°C at a metabolic rate of 1.2 met and a clothing profile for summer indoor. At first, the pressure is set at sea level value and the relative humidity is set at 70 percent. Secondly, the pressure is maintained at sea level value whereas the relative humidity is significantly lowered to 15 percent. Finally, the pressure is lowered to a cabin altitude of 8000 feet and the relative humidity is maintained at 15 percent. The predicted variation of skin temperatures for these three different environmental conditions is depicted in Fig. 14.

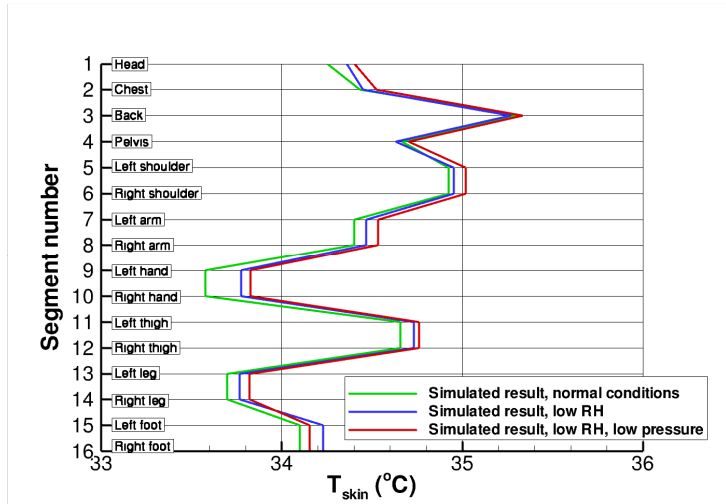


Figure 14. Comparison of simulated results for segmental skin temperatures for normal, dry, and low-pressure conditions.

The predicted variation of skin temperatures for these three different environmental conditions is depicted in Fig. 14. The associated values for the core temperature are 36.87°C , 36.87°C and 36.84°C respectively, and for the average skin temperature 34.47°C , 34.52°C and 34.57°C respectively.

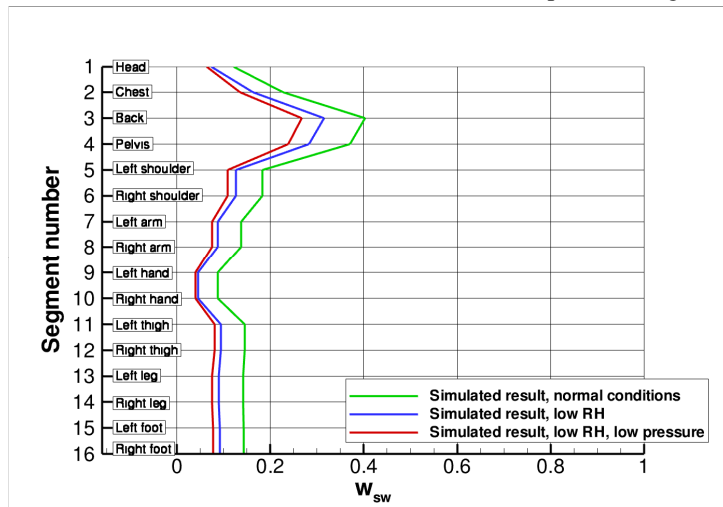


Figure 15. Comparison of simulated results for segmental skin wettedness for normal, dry, and low-pressure conditions.

The maximum segmental variation is predicted to be limited to about 0.25°C , which clarifies the difficulty to observe such changes on the basis of infrared camera recordings. As an additional visualisation of simulated results, the impact of these conditions on skin wettedness is shown in Fig. 15. It is observed that the skin wettedness decreases, especially with the reduction in relative humidity. The reduction of cabin pressure gives an additional, yet smaller reduction on skin wettedness values. Although the basal skin wettedness drops in a dry environment, it has been noted before that the active perspiration control mechanism is likely to compensate for this reduction. Since the heat exchange

mechanisms within the aircraft cabin environment change with pressure and relative humidity variations, it is still possible that the perception of the environment becomes different. For this purpose, the impact of the relative humidity and pressure changes on the different heat exchange terms of the bio-heat equation are visualized in Fig. 16. It is shown that the skin diffusion term significantly drops due to the low relative humidity, but this change is counteracted by the perspiration term at sea level or by the latent respiratory heat loss at altitude. Convection is reduced at altitude, which is in part taken over by the latent respiratory heat loss. Thus, the main result is that skin diffusion is reduced in low relative humidity conditions, whereas the pressure impact is mainly to be found in the latent respiratory heat loss and the convection. Radiative heat loss increases a bit at lowered cabin pressure due to

the slightly higher resulting skin temperatures. It should be noted that other shifts are possible when using different clothing profiles or different environmental conditions.

What the 65-node thermoregulation model is actually showing is that, within the normal operational range of aircraft cabin pressure and humidity, the impact of these parameters on thermal comfort is found to be limited, but the heat exchange variations could imply a change in perception of cabin comfort. For instance, the increase in latent respiratory heat loss could be linked to the occurrence of a dry throat³⁴, whereas the increase of the perspiration term in dry environments as a result of the active control mechanisms could result in a reduced feeling of well-being.

A further attempt to specify the impact of pressure and relative humidity on thermal comfort in aircraft cabins is based on comfort votes. From the experiments within the ICE-project^{11,12}, especially the part of the experiments that has been performed in the Flight Test Facility (FTF) at the Institute of Building Physics (IBP) of the Fraunhofer Institute in Valley, Germany, data have been obtained from groups of test persons exposed to simulated flights in a pressurized aircraft cabin with controlled pressure and relative humidity variations. The analysis of thermal votes obtained in this way has resulted in correlations, predicting the percentage of people dissatisfied (*PPD*) with temperature, pressure, relative humidity and so on. Although information on a vast number of variables has been obtained in the experiments, here only the resulting pressure and relative humidity correlations are considered. It has been found from the experiments, when cabin altitude is increased and thus pressure is decreased, that the percentage of people dissatisfied with the temperature decreases, based on answers in the range between ‘too cool’ to ‘comfortable’ (denoting a cool or blue branch). The average *PPD* for the overall satisfaction with temperature has been correlated with altitude according to the curve in Fig. 17, with the cabin altitude in feet, limited to the range between 0 and 8000 ft. This correlation shows that the *PPD* for the overall satisfaction with temperature is never larger than 21 percent, and is about 4 percent at 8000 ft. Since the results are obtained from a cool branch, a decrease in *PPD* is equivalent to an increase in *PMV*,

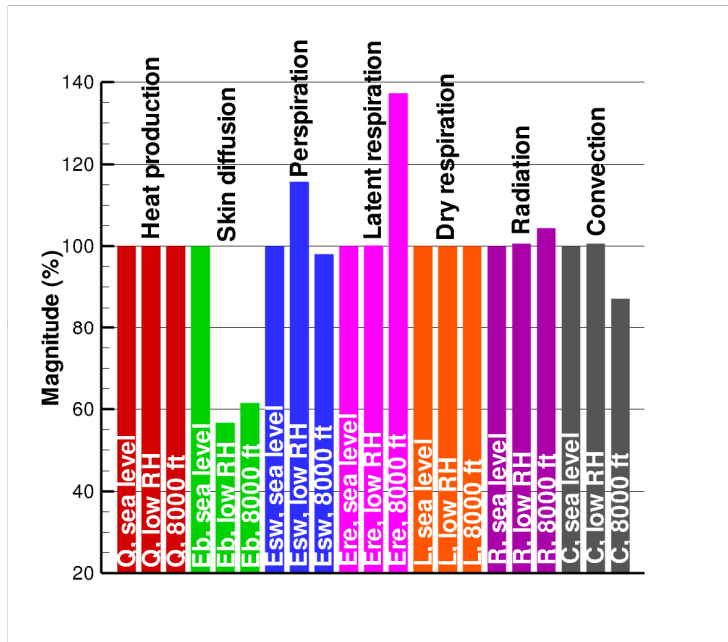


Figure 16. Relative variation of individual terms of the bio-heat equation, summed over the body segments, for simulated results using the clothing profile for summer indoor.

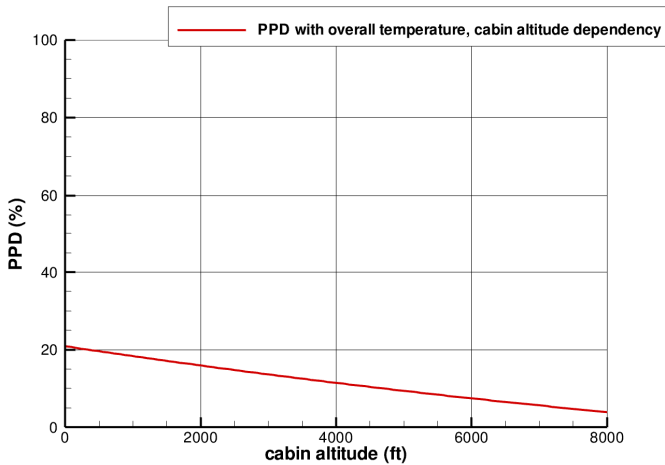


Figure 17. Correlation of *PPD* for the average overall satisfaction with temperature as function of cabin altitude, correlation from FTF-experiments.

see e.g. a normative reference⁴. Thus, an increase in cabin altitude results in a higher thermal vote. Another correlation obtained from the experiments is shown in Fig. 18 for the *PPD* with air quality as function of the relative humidity. This figure shows that the percentage of people dissatisfied with the dryness of the air increases with decreasing relative humidity. A maximum of about 56 percent is obtained for very low relative humidity. It should

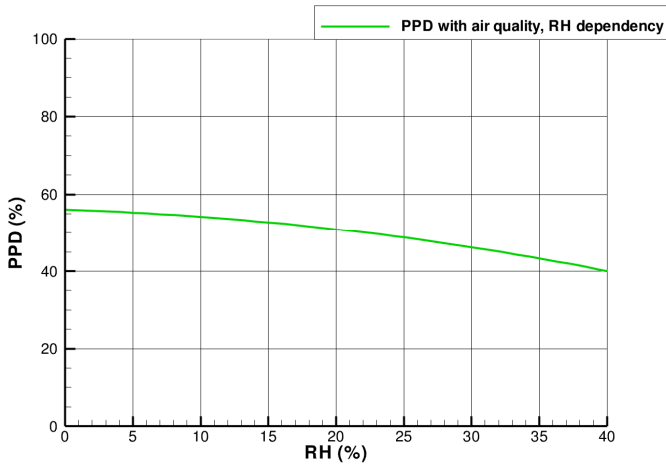


Figure 18. Correlation of PPD for the average satisfaction with air quality as function of RH, correlation from FTF-experiments.

somewhat lower than the experimentally observed value of about 15 percent, which might be linked to the fact that the experimental correlation shown in Fig. 17 is only accounting for the cold branch (some people might become dissatisfied with the increase in thermal sensation, i.e. the hot branch of the PPD-curve, thereby reducing the decrease in PPD).

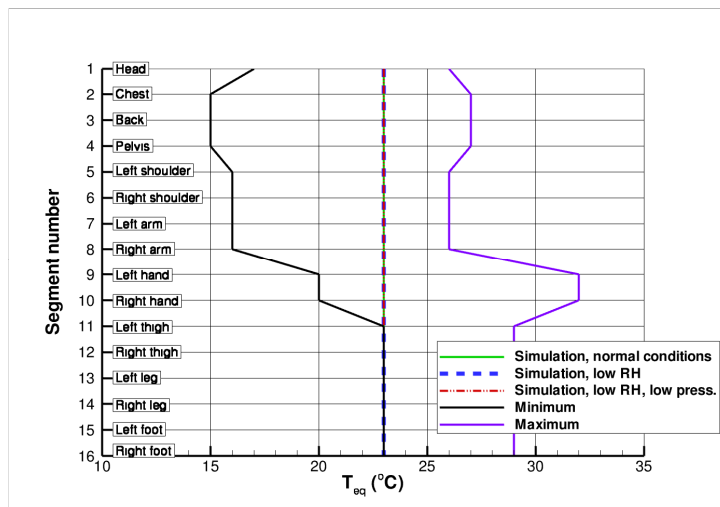


Figure 19. Equivalent temperature evaluation per body segment in uniform conditions for the assessment of local comfort.

temperature per segment, together with the claimed limits of local comfort^{26,27}, see Fig. 19. According to Ref. 35, the equivalent temperature is “the uniform temperature of the imaginary enclosure with air velocity equal to zero in which a person will exchange the same dry heat by radiation and convection as in the actual non-uniform environment”. By visualizing the equivalent temperature per body segment in this way, an impression is obtained of the local comfort of body segments in a non-uniform environment. This is especially useful when temperature gradients exist in the cabin, either vertically or horizontally. In the current simulations, no temperature gradients were applied and a uniform environment is assumed, resulting in an identical equivalent temperature over all body segments. As shown in Fig. 19, the change in relative humidity and cabin pressure does not impact the equivalent temperature based on the dry heat exchange due to radiation and convection. Thus, within these three different environmental conditions, a result for the local comfort is obtained that is acceptable for all body segments. For a specific enhancement of this type of visualization of predicted results for aircraft cabin environments, a similar plot showing the skin wettedness per body segment (as in Fig. 15) together with associated minimum and maximum

be noted that no flights with a relative humidity larger than 40 percent have been performed, although the trend suggests that the PPD will drop to lower values for higher relative humidity values.

The experimentally obtained correlations are supported by the trends in the results of the 65-node thermoregulation model. A small increase in the predicted thermal vote with altitude is obtained, thereby reducing the number of people still experiencing a too cold temperature. A similar increase in the predicted thermal vote is obtained when lowering the relative humidity, which changes the heat exchange with the environment to different terms of the bio-heat equation. The overall increase in thermal sensation vote from the 65-node thermoregulation model is about 0.2, which could be related to a decrease in PPD of about 8 percent⁴. This decrease in PPD is reflected in the experimentally obtained percentage of people dissatisfied with the air quality as shown in Fig. 18. Although the 65-node thermoregulation model does not provide an output parameter of air quality sensation in this respect, the increase in perspiration and in latent respiratory heat loss for low relative humidity and low pressure conditions, respectively, is easily understood in a decreased feeling of comfort with the air quality.

Finally, following a local comfort data presentation approach from the automotive industry, the results of the 65-node thermoregulation model for the environmental conditions as used in Fig. 14 and Fig. 15 are shown in terms of equivalent

limits is proposed, to be used in combination with the segmental equivalent temperature plot. For this purpose, the minimum and maximum comfort boundaries for acceptable skin wettedness per body segment need to be developed. The minimum is likely to be close to 0.06 (the normal basal skin wettedness) whereas the maximum is expected to lie around 0.2 for clothed body segments.

V. Conclusion

The 65-node thermoregulation model of Tanabe, describing the thermal response of an average person, has been enhanced to model the impact of cabin air pressure and humidity on thermal comfort. For this purpose, relations in the model have been adjusted, and an appropriate correlation of predicted model temperatures with thermal votes has been added. Validation of the model with objective data (measured temperature distributions) and subjective data (thermal votes) has been shown on the basis of a range of available data. The specific impact of aircraft cabin pressure and relative humidity on thermal comfort has been studied in relation to available information from simulated flights with controlled parameters in a flight test facility. It is observed that, for the common operational range of cabin pressure and relative humidity in aircraft cabins, the impact of these parameters on temperature distributions over the body is limited, whereas a small increase of thermal comfort votes (a decrease of the number of people dissatisfied with a too cold environment) with higher cabin altitude is predicted. These findings are supported by experimentally obtained correlations.

This does not imply that the impact of pressure and humidity on thermal comfort in aircraft cabins can be completely ignored. The shift of heat exchange between the passenger and the environment to different mechanisms can result in a change of perception of well-being by passengers, such as sensations of dry mouth and changes in perspiration. Studies related to the definition of the optimum cabin environment should focus on such perception issues, and how they can be influenced by ventilation optimization, air recirculation, and so on. The enhanced thermoregulation model is a suitable tool to support such studies, either as a stand-alone thermal comfort indicator or in a coupled mode with a CFD-method for the cabin air flow.

Acknowledgments

The research outlined in this paper has been performed with 50 percent funding by the European Committee, and 50 percent funding from NLR's programmatic research "Kennis als Vermogen". The contributions of the following people and organizations are gratefully acknowledged: former colleague H.S. Dol in setting up the calculation routine for the basic 65-node thermoregulation model, professor S. Tanabe and his master student T. Sato from Waseda University of Tokyo for their kind help in checking the correctness of the implemented model, colleague J.C. Kok for coupling of the 65-node model in a CFD-environment, master student S.S. Burgers for contributing to the development of the enhanced model, the European partners in the Friendly Aircraft Cabin Environment (FACE) and Ideal Cabin Environment (ICE) projects, and finally the European Committee by granting the FACE and ICE projects.

References

- ¹American Society of Heating, Refrigerating and Air-Conditioning Engineers, "Air Quality within Commercial Aircraft", *ASHRAE Standard 161-2007*, May 2008.
- ²European Committee for Standardization, "Aerospace Series – Aircraft Internal Air Quality Standards, Criteria and Determination Methods", *CEN EN 4618:2009*, September 2009.
- ³Fanger, P.O., *Thermal Comfort, Analysis and Applications in Environmental Engineering*, McGraw-Hill, New York, 1972.
- ⁴International Organization for Standardization, "Ergonomics of the Thermal Environment – Analytical Determination and Interpretation of Thermal Comfort using Calculation of PMV and PPD Indices and Local Thermal Comfort Criteria", *ISO 7730*, 3rd Edition, 2005.
- ⁵Doherty, T., and Arens, E.A., "Evaluation of the Physiological Bases of Thermal Comfort Models", *Centre for the Built Environment, University of California, Berkeley*, 1988.
- ⁶Stolwijk, J.A.J., "A Mathematical Model of Physiological Temperature Regulation in Man", *NASA CR-1855*, 1971.
- ⁷Tanabe, S., Kobayashi, K., Nakano, J., Ozeki, Y., and Konishi, M., "Evaluation of Thermal Comfort Using Combined Multi-Node Thermoregulation (65MN) and Radiation Models and Computational Fluid Dynamics (CFD)", *Energy and Buildings* Vol. 34, 2002, pp. 637-646.
- ⁸International Organization for Standardization, "Ergonomics of the Thermal Environment – Evaluation of Thermal Insulation and Water Vapour Resistance of a Clothing Ensemble", *ISO 9920*, 2007.
- ⁹Park, S., and Hellwig, R., "Comparison of Two Different Calculation Principles for Determining the Thermal Insulation of Clothing", *Indoor Air Conference 2008*, Copenhagen, Denmark, 17-22 August 2008.

¹⁰Kok, J.C., Muijden, J. van, Burgers, S.S., Dol, H., and Spekrijse, S.P., "Enhancement of Aircraft Cabin Comfort Studies by Coupling of Models for Human Thermoregulation, Internal Radiation, and Turbulent Flows", *ECCOMAS CFD Conference*, Egmond aan Zee, The Netherlands, 5-8 September 2006.

¹¹Bagshaw, M., "Comfort and Well-Being – The Influence of Cabin Altitude", *ICE International Aviation Conference*, Munich, Germany, 9-10 March 2009.

¹²Grün, G., Holm, A.H., Luks, N., Malone-Lee, J., Trimmel, M., Schreiber, R., and Mellert, V., "Impact of Cabin Pressure on Aspects of the Well-Being of Aircraft Passengers – A Laboratory Study", *26th International Congress of the Aeronautical Sciences (ICAS)*, Anchorage, Alaska, 14-19 September 2008.

¹³Muhm, J.M., Rock, P.B., McMullin, D.L., Jones, S.P., Lu, I.L., Eilers, K.D., Space, D.R., and McMullen, A., "Effect of Aircraft-Cabin Altitude on Passenger Discomfort", *The New England Journal of Medicine*, Vol. 357, No. 1, 5 July 2007, pp. 18-27.

¹⁴International Organization for Standardization, "Standard Atmosphere", *ISO 2533:1975*, 1975.

¹⁵Arens, E., and Zhang, H., "The Skin's Role in Human Thermoregulation and Comfort", *Thermal and Moisture Transport in Fibrous Materials*, edited by N. Pan and P. Gibson, Woodhead Publishing Ltd., Cambridge, England, 2006, pp. 560-602.

¹⁶Gonzalez, R.R., and Cena, K., "Evaluation of Vapor Permeation through Garments during Exercise", *Journal of Applied Physiology*, Vol. 58, No. 3, 1985, pp. 928-935.

¹⁷Shavit, A., and Gutfinger, C., *Thermodynamics: from Concepts to Applications*, 2nd edition, Prentice Hall, London, 1995.

¹⁸Kreith, F., and Black, W.Z., *Basic Heat Transfer*, Harper and Row, New York, 1980.

¹⁹Chang, S.K.W., and Santee, W.R., "Clothing Insulation in a Hypobaric Environment", *Aviation, Space, and Environmental Medicine*, Vol. 67, No. 9, September 1996, pp. 827-834.

²⁰Dear, R. de, Arens, E., Hui, Z., and Oguro, M., "Convective and Radiative Heat Transfer Coefficients for Individual Human Body Segments", *International Journal of Biometeorology*, Vol. 40, 1997, pp. 141-156.

²¹Brake, D.J., "The Deep Body Core Temperatures, Physical Fatigue and Fluid Status of Thermally Stressed Workers and the Development of Thermal Work Limit as an Index of Heat Stress", *PhD. Thesis*, Curtin University of Technology, Australia, 2002.

²²McIntyre, D.A., *Indoor Climate*, Applied Science Publishing, 1980.

²³Havenith, G., Holmer, I., Hartog, E.A. den, and Parsons, K.C., "Clothing Evaporative Heat Resistance – Proposal for Improved Representation in Standards and Models", *Annual Occupational Hygiene*, Vol. 43, No. 5, 1999, pp. 339-346.

²⁴International Organization for Standardization, "Hot Environments – Analytical Determination and Interpretation of Thermal Stress using Calculation of Required Sweat Rate", *ISO 7933*, 1989.

²⁵Kozak, T., and Majchrzycka, A., "The Influence of Pressure on Permeation Efficiency Factor for Vapour Transfer", *Marine Technology IV*, Wessex Institute of Technology, UK, 2001.

²⁶Han, T., and Huang, L., "A Model for Relating a Thermal Comfort Scale to EHT Comfort Index", *SAE Paper 2004-01-0919*, 2004.

²⁷Curre, J., "Numerical Simulation of the Flow in a Passenger Compartment and Evaluation of the Thermal Comfort of the Occupants", *SAE Paper 970529*, 1997.

²⁸Fiala, D., "Dynamic Simulation of Human Heat Transfer and Thermal Comfort", *PhD. Thesis*, De Montfort University, Leicester, UK, and Fachhochschule Stuttgart, Germany, June 1998.

²⁹Boregowda, S.C., Tiwari, S.N., Chaturvedi, S.K., Hou, G.J.W., and Morris, J.D., "Numerical Simulation of Human Thermoregulation in Different Environmental Conditions", *AIAA Paper 97-0137*, 1997.

³⁰Ooijen, A.M.J. van, Marken Lichtenbelt, W.D. van, Steenhoven, A.A. van, Westerterp, K.R., "Seasonal Changes in Metabolic and Temperature Responses to Cold Air in Humans", *Physiology and Behavior*, Vol. 82, 2004, pp. 545-553.

³¹Fiala, D., Lomas, K.J., and Stohrer, M., "Computer Prediction of Human Thermoregulatory and Temperature Responses to a Wide Range of Environmental Conditions", *International Journal of Biometeorology*, Vol. 45, 2001, pp. 143-159.

³²Nilsson, H.O., "Comfort Climate Evaluation with Thermal Manikin Methods and Computer Simulation Models", *Arbete og Hälsa*, No. 2004:2, Stockholm, Sweden, 2004.

³³Zhang, H., "Human Thermal Sensation and Comfort in Transient and Non-Uniform Thermal Environments", *PhD. Thesis*, University of California, Berkeley, 2003.

³⁴Ree, H. de, Bagshaw, M., Simons, R., and Brown, R.A., "Ozone and Relative Humidity in Airline Cabins on Polar Routes: Measurements and Physical Symptoms", *Air Quality and Comfort in Airliner Cabins*, *ASTM STP 1393*, edited by N.L. Nagda, American Society for Testing and Materials, West Conshohocken, Pennsylvania, 2000.

³⁵International Organization for Standardization, "Ergonomics of the Thermal Environment – Evaluation of Thermal Environments in Vehicles – Part 2: Determination of Equivalent Temperature", *ISO 14505-2*, 2006.